WIRELESS COMMUNICATIONS AND MOBILE COMPUTING
Wirel. Commun. Mob. Comput. 2012; **12**:713–728
Published online 1 July 2010 in Wiley Online Library (wileyonlinelibrary.com). DOI: 10.1002/wcm.1008

RESEARCH ARTICLE

MCR: MAC-assisted congestion-controlled routing for wireless multihop networks†

Yu-Pin Hsu[1] and Kai-Ten Feng[2]

[1] Department of Electrical and Computer Engineering, Texas A&M University, College Station, TX, U.S.A.
[2] Department of Electrical Engineering, National Chiao Tung University, Hsinchu, Taiwan, Republic of China

ABSTRACT

Techniques for improving network congestion have been proposed in different fields. In recent years, the congestion control problems were studied to enhance the routing performance in wireless multihop networks (WMNs). In this paper, the network allocation vector (NAV) introduced by the contention-based medium access control (MAC) protocols is utilized for the determination of the channel status around a wireless node (WN). A MAC-assisted congestion-controlled routing (MCR) algorithm is proposed to alleviate the network congestion problem by adopting the information from the MAC layer. The routing path is selected based on the congestion-free probability along the path for transmitting the data packets. Moreover, the adaptive path-switching scheme and the aggressive hop-reduction (AHR) local repair mechanism further enhance the routing performance of the proposed MCR algorithm. The effectiveness of the MCR protocol is evaluated *via* both the analytical study and the simulation results. Without consuming excessive control packets for each WN, the MCR algorithm can achieve better performance when compared with other existing schemes, especially under the scenarios with network congestion. Copyright © 2010 John Wiley & Sons, Ltd.

KEYWORDS

congestion control; routing protocol; contention-based medium access control; wireless multihop networks

***Correspondence**

Kai-Ten Feng, Department of Electrical Engineering, National Chiao Tung University, Hsinchu, Taiwan, Republic of China.
E-mail: ktfeng@mail.nctu.edu.tw

1. INTRODUCTION

The wireless multihop network (WMN) has attracted a significant amount of attention in recent years. A WMN consists of wireless nodes (WNs) that can cooperate to each other for various purposes such as coverage enlargement [1], diversity enhancement [2], and event detection [3]. Due to the distributed nature of WMNs, the available resources for each WN are considered limited for most of the current applications. How to provide an efficient multihop routing protocol has become an important issue for the design of WMNs. Different types of multihop routing algorithms have been developed, which can be categorized into the proactive (e.g., destination-sequenced distance-vector (DSDV) routing [4]) and the reactive schemes (e.g., *ad hoc* on-demand distance vector (AODV) routing [5] and dynamic source routing (DSR) [6]). However, these protocols may lead to poor routing performance (e.g., low packet delivery ratio and high end-to-end delay) due to potential network congestion within certain areas of the WMN. Therefore, it will be difficult to guarantee persistent routing performance or quality-of-service within the WMNs.

In order to improve the multihop routing performance, several congestion control techniques have been investigated in [7–10]. The dynamic codeword routing (DCR) [7] proposed a codeword conceptual model to balance the total traffic load within the network. The load-balanced *ad hoc* routing (LBAR) [8] and the dynamic load-aware routing (DLAR) [9] schemes consider the number of interfering routes around a WN in order to determine if this WN should be selected as a forwarding node within the route. The routing with minimum contention time and load balancing (MCL) [10] algorithm determines its route selection criterion based on the total number of contenting nodes around the neighborhood of a WN, which improves the routing performance with the occurrence of network congestion. Most of the existing load-balancing routing schemes measure the degree of network congestion by gathering the neighboring

† Part of this manuscript has been submitted as a conference paper and was nominated as a candidate for the Best Student Paper Award in the IEEE Radio and Wireless Symposium (RWS) 2008.

information *via* the utilization of additional control packets. However, the resulting extravagant control overhead is considered unfavorable for the resource-limited WMNs.

In order to reduce the excessive usage of the control packets within the network layer, the information acquired from the medium access control (MAC) layer can be incorporated within the routing protocol design. The cross-layer designs for multihop routing algorithms have been investigated from various aspects [11–16]. The work proposed in Reference [11,12] theoretically formulates the network congestion as an utility optimization problem with cross-layer constraints, while Cao *et al*. [12] additionally takes the power-saving issue into consideration. Moreover, the location-aided proactive routing with congestion control is proposed in Reference [13]. Either additional network nodes [14,15] or multiple intelligent agents [14] are suggested across the network that cooperate with each other in order to find the congestion-relieved routes between the source and destination. Both a zone manager and border routers are utilized in Reference [15] for a zone-based congestion detection. It is noticed that additional assistance from specific nodes or positions information are required for these types of congestion control algorithms. Furthermore, [16] adopts two metrics for the purpose of reflecting network congestion, i.e., the average MAC layer utilization and the queue length. However, similar to the LBAR scheme, excessive control overheads are required in Reference [14,16] for the accumulation of neighboring information. Therefore, the intend of the this paper is to alleviate the network congestion problem based on the cost-free information adopted from the MAC layer without inducing excessive overhead in the network layer protocol.

In this paper, a MAC-assisted congestion-controlled routing (MCR) protocol is proposed in order to alleviate the network congestion based on the channel information adopted from the MAC layer. Instead of generating control packets to obtain the desired information from the network neighbors, the proposed MCR scheme utilizes the existing information, i.e., the network allocation vector (NAV), from the request-to-send (RTS) and the clear-to-send (CTS) packets within the MAC layer. The channel-free probability, which is computed from the NAV vectors of the WN, is carried within the route discovery processes to determine the feasible route for packet delivery. It is noticed that the information inherently considers different data rates, data sizes, and the number of interfering neighbors that may occur within the various routes. The proposed MCR scheme can also adaptively switch between the selected paths while the level of network congestion has been changed. Moreover, an aggressive hop-reduction (AHR) local repair scheme is employed within the MCR algorithm, which can reconnect the broken communication links with reduced number of forwarding WNs. The MCR scheme can improve the network congestion problem without the extravagant usage of control packets. The effectiveness of the MCR algorithm will be validated *via* both the analytical study and the simulation results.

The rest of this paper is organized as follows. Section 2 briefly reviews the LBAR routing algorithm and the IEEE 802.11 MAC protocol. The proposed MCR scheme is explained in Section 3. Section 4 provides the analytical studies of the MCR algorithm. Section 5 illustrates the performance evaluation of the MCR scheme *via* both the analytical and the simulation results. Section 6 draws the conclusions.

2. PRELIMINARIES

In order to facilitate the design of the proposed MCR algorithm, the LBAR routing scheme and the IEEE 802.11 MAC protocol are briefly summarized as follows.

2.1. LBAR protocol

Similar to the AODV protocol in Reference [5], the LBAR scheme [8] is also a reactive algorithm which conducts route request/reply (RREQ/RREP) cycles for route discovery. The path cost, which considers the number of interfering paths around the forwarding WN, is carried along with the RREQ packets in the LBAR scheme. An appropriate path is selected by the destination node with minimum cost, which is defined as

$$\Omega_\kappa = \sum_{i \in \kappa} (\omega_i + \zeta_i) \tag{1}$$

where Ω_κ denotes the cost along the path κ; ω_i is the number of active paths through node i, where i represents a WN on the path κ. ζ_i indicates the traffic interference as $\zeta_i = \sum_{\forall j} \omega_j^i$, which is the activity sum of the neighbors around node i. We recall that ω_j^i denotes the active paths at node j, which is a neighbor WN of node i. It is worthwhile to notice that the hello packets are adopted for the exchange of ω_i within the LBAR scheme, which will be foreseeable to induce excessive control packets.

2.2. IEEE 802.11 MAC protocol

Owing to the well-adopted capability for collision avoidance, the IEEE 802.11 MAC protocol [17] is exploited within the design of WMNs. The distributed coordination function (DCF) is utilized as the basic access mechanism in the IEEE 802.11 MAC protocol. The DCF is based on the carrier sensing multiple access with collision avoidance (CSMA/CA) scheme to ensure that each WN can acquire a fair chance to access the wireless medium. A random backoff process is executed in each WN for the purpose of decreasing the probability of data collision. Moreover, the RTS/CTS exchange before the data transmission is exploited to resolve the potential hidden terminal problem. In order to avoid packet collision during data transmission, the virtual carrier sensing mechanism carried out by the

NAV vector is utilize to record the duration of the ongoing data transmission. We recall that the NAV information associated within a WN will be delivered to its neighbor nodes. A non-zero NAV value recorded in a WN will consequently prohibit the surrounding neighbor nodes to initiate a new data transmission.

3. PROPOSED MCR PROTOCOL

The main objective of the proposed MCR algorithm is to alleviate the network congestion problem without the extravagant usage of control packets by exploring the useful and gratuitous information from the MAC layer. For each specific source and destination pair (S_i, D_i), the set of available paths for packet delivery can be defined as

$$\mathbf{P}_i \triangleq \{\boldsymbol{p}_{i,j} \mid \boldsymbol{p}_{i,j} = [F_{i,j,1}, \ldots F_{i,j,k}, \ldots, F_{i,j,N_j}], \forall i, 1 \leq j \leq l_i, N_j\} \quad (2)$$

We recall that $\boldsymbol{p}_{i,j}$ corresponds to the jth delivering path associated with the (S_i, D_i) pair, and is composed by a set of forwarding nodes $F_{i,j,k}$. The parameter l_i denotes the total number of available routing paths between S_i and D_i; and N_j represents the number of forwarding nodes $F_{i,j,k}$ within the jth path. The notations as defined above will be utilized in the remaining subsections for the design of the proposed MCR algorithm. In subsection 3.1, the channel-free probability is introduced. The route discovery process and the adaptive path-switching scheme within the proposed MCR protocol are explained in subsection 3.2. The AHR local repair mechanisms are described in subsection 3.3, while subsection 3.4 briefly depicts the implementation issue of the MCR algorithm.

3.1. Channel-free probability of considered path

The channel-free probability is adopted as the criterion for path selection within a route. The value recorded within the NAV vector is utilized to determine the channel idle probability. It is noticed that the NAV vectors within a WN are employed to indicate if the channel is busy with packet transmission. There are four kinds of NAV values in each WN that are, respectively, updated by the RTS packet (N_r), the CTS packet (N_c), the data packet (N_d), and the ACK packet (N_a). Each value represents the remaining time duration until the corresponding data packet has finished its transmission. A WN is considered to possess idle channel status as all its NAV vectors become zero. Since (a) the NAV value set by the data packet generally overlaps with that determined from the RTS packet and (b) the NAV value determined by the ACK packet is zero in the common non-fragmentation schemes [17], their effects on the channel status are neglected in this paper.

Figure 1(a) illustrates the schematic diagram for the network topology with two transmission paths from S_1 to D_1, i.e., $\boldsymbol{p}_{1,1}$, and from S_2 to D_2, i.e., $\boldsymbol{p}_{2,1}$. The packets sent from all the WNs in Figure 1(a) are depicted in their respective timelines as in Figure 1(b), where the RTS/CTS-based collision avoidance scheme with their associated NAV vectors are illustrated. It is assumed that node X represents an intermediate node within $\boldsymbol{p}_{1,1}$, while node Y belongs to the path $\boldsymbol{p}_{2,1}$ for packet transmission. It is also considered that smaller data rate and data size are employed in the path $\boldsymbol{p}_{1,1}$ in comparison with that in $\boldsymbol{p}_{2,1}$. Node Z, which resides within the communication ranges of nodes X and Y, will consequently be assigned with various NAV vectors due to the packet transmissions from both paths. The combined NAV vectors, observed within node Z, are shown in the last timeline in Figure 1(b). It can be obtained that the accumulated NAV vectors at node Z implicitly contain the mixed effects from both the data rate and the data size of the transmitted packets, i.e., node X with smaller data rate and size as compared to that from node Y.

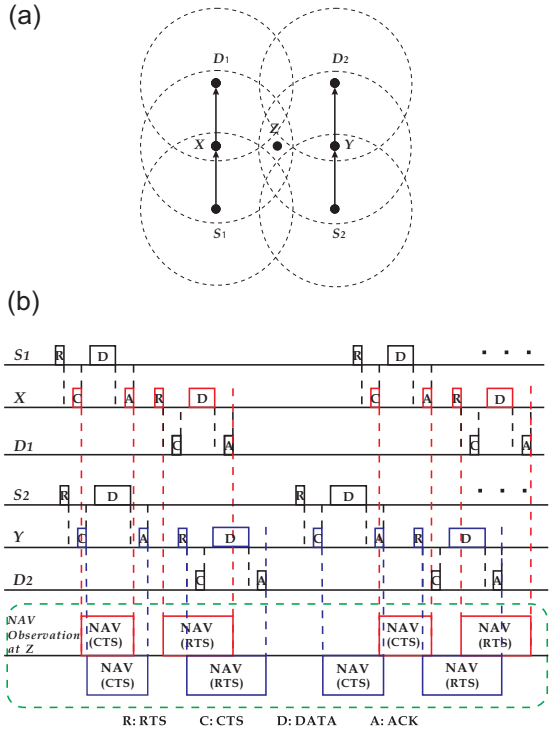

Figure 1. Schematic diagrams of (a) an exemplified network topology and (b) the RTS/CTS-based collision avoidance scheme associated with the NAV vectors.

In the IEEE 802.11 protocol, the time scale is slotted with the slot time length denoted as σ, which is set equal to the time required for a WN to detect the transmission of a packet from its neighbor nodes. The σ value is primarily determined based on the physical layer design, e.g., $\sigma = 20\,\mu$s in the direct sequence spread spectrum (DSSS), and $\sigma = 50\,\mu$s in the frequency hopping spread spectrum (FHSS). A set of random variables $\boldsymbol{X} = \{\mathcal{X}_i\}$ is utilized to represent the channel condition in each time slot i, where $\mathcal{X}_i = 1$ denotes that the slot is in the busy state, and $\mathcal{X}_i = 0$ indicates the idle state. The random variable $\mathcal{X}_i$ can be

represented by conducting binary union operation on indicator functions as

$$\mathcal{X}_i = \bigcup_{\forall p} \mathbf{I}_{i,N_r(p)} \bigcup_{\forall q} \mathbf{I}_{i,N_c(q)} \tag{3}$$

where the indicator functions $\mathbf{I}_{i,N_r(p)}$ and $\mathbf{I}_{i,N_c(q)}$ are defined as

$$\mathbf{I}_{i,N_r(p)} = \begin{cases} 1, & \text{if the } p\text{th RTS NAV value} N_r(p) \\ & \text{covers slot } i \\ 0, & \text{otherwise} \end{cases} \tag{4}$$

$$\mathbf{I}_{i,N_c(q)} = \begin{cases} 1, & \text{if the } q\text{th CTS NAV value } N_c(q) \\ & \text{covers slot } i \\ 0, & \text{otherwise} \end{cases} \tag{5}$$

It is noted from Figure 1(b) that different situations can occur within the network, e.g., overlapped N_r and N_c, or stand alone N_r and N_c. Then, we measure the channel-busy probability $P_k^B(t)$ of a node k at the time slot t as shown Equation (6) *via* the sample average adopted from time slot $t-n$ to t.

$$P_k^B(t) \triangleq \frac{1}{n} \sum_{i=t-n}^{t} \mathcal{X}_i \approx \frac{\Delta T_k^B(t)}{\Delta T} \tag{6}$$

Note that n in Equation (6) is not restricted to a single NAV duration induced by its corresponding transmission. Instead, it represents a longer time interval as an average of the observed channel quality, i.e., either busy or idle. In other words, the variables $\mathcal{X}_i$s that indicate the channel condition for each time slot to compute $P_k^B(t)$ in Equation (6) are not confined within a single NAV duration. Therefore, the intent of Equation (6) is to utilize the time average value in order to measure the channel status. The current channel-busy probability is calculated according to samples in the past n samples, i.e., by means of the sliding window with the window size of n. Furthermore, the second equality of Equation (6) transforms the observed sliding window into time scale, where $\Delta T = n \cdot \sigma$ and $\Delta T_k^B(t)$ indicate the total duration of the busy state of node k within the period $(t - \Delta T, t)$. The channel busy probability can, therefore, be calculated by taking union on all the NAV information within the observation time ΔT. This shows the major concept by adopting the NAV messages to facilitate the design of proposed congestion controlled routing algorithm.

For simplicity, the notation $P_k^B(t)$ is shorten as P_k^B in the remaining parts of the paper. The major assumption for measuring the network congestion is to consider the ergodic traffic environment. In other words, we try to associate the time averages with the ensemble averages. Although the ergodicity assumption may not be practical, the average value from several observations will be helpful in figuring out the potential network congestion status at present. The main point of the proposed metrics in Equation (6) is to take into account the mixed effect from various data rate/size and the number of neighbors without introducing excessive control packets. The average behavior in terms of time in Equation (6) provides a more stable metrics for the measurement of network congestion level under varying traffic.

The feasible value of n will further be determined in subsection 5.1. It is worthwhile to notice that the channel busy probability P_k^B inherently combines the effects from the following: (a) the data rate and data size of the transmitted packets and (b) the number of the interfering neighbor nodes. For instance, the longer duration obtained from $\Delta T_{N_r(p)}$ in Equation (6) indicates that its corresponding data packet has a larger data size to be transmitted, which will result in a higher value of P_k^B in Equation (6). Furthermore, the number of interfering nodes and the data rate for a specific set of data packets depend on the occurring frequency of their corresponding $N_r(p)$ (or $N_c(q)$). As a result, the information of network traffic can be acquired from Equation (6) by exploiting the cross-layer information, i.e., by observing the NAV vectors that are updated by the corresponding RTS and CTS packets. The situation of network congestion can consequently be detected without the utilization of additional control packets. Moreover, the channel idle probability for node k can also be acquired as

$$P_k^I = 1 - P_k^B \tag{7}$$

In the proposed MCR scheme, the criterion for selecting a feasible routing path is determined by the maximum channel-free probability of the path $\boldsymbol{p}_{i,j}$, which is defined as

$$P_{\boldsymbol{p}_{i,j}} \triangleq \prod_{k=1}^{N_j} P_{F_{i,j,k}}^I = P_{F_{i,j,1}}^I \ldots P_{F_{i,j,k}}^I \ldots P_{F_{i,j,N_j}}^I \tag{8}$$

It is noticed that Equation (8) is proposed and defined as a criterion for the selection of a feasible routing path. It represents an upper bound of congestion free probability along the path, which is computed as the product of channel idle probabilities. Since the channel idle probability between the nodes along the path may not be always independent of each other, the true congestion free probability along the path should be less than or equal to $P_{\boldsymbol{p}_{i,j}}$. Moreover, the channel idle probability $P_{F_{i,j,k}}^I$ in Equation (8) for each forwarding node $F_{i,j,k}$ can be obtained from Equation (7). It is noticed that the channel idle probabilities of the source node (i.e., $P_{S_i}^I$) and the destination node (i.e., $P_{D_i}^I$) are excluded in the criterion since the paths $\boldsymbol{p}_{i,j}$ (for all j) share the same (S_i, D_i) pair. The processes for acquiring the channel-free probability $P_{\boldsymbol{p}_{i,j}}$ from each intermediate WN will be explained in the next subsection.

3.2. Route discovery process and adaptive path-switching scheme

The proposed MCR scheme is considered a cross-layer based approach since it incorporates the NAV information

from MAC layer into the routing decision in network layer for the alleviation of network congestion. In other words, the channel-busy probability of each node k in Equation (6) is adopted by exploiting the cross-layer information from the observation of the NAV vectors that are updated by their corresponding RTS and CTS packets. The main concept of the proposed criterion in Equation (6) is to take into account the mixing effect from various data rate/size and the number of neighbors. Therefore, we can construct a less congested route from the cross-layer information without introducing excessive control packets that frequently occur if traffic information is exchanged within the network layer.

The route discovery process of the proposed MCR algorithm is a modified version based on the conventional AODV *ad hoc* routing protocol [5]. Each WN within the MCR scheme maintains a routing table, which contains the following information: (a) the next hopping node, (b) the next two-hopping node, (c) the sequence number, (d) the hop counts, and (e) the channel-free probability $P_{\boldsymbol{p}_{i,j}}$. It is noted that the information of the next two-hopping node is utilized in the AHR scheme, which will be discussed in the next subsection.

It is considered that the source node S_i intends to send data packets to the destination node D_i. *via* some of the forwarding nodes $F_{i,j,k}$. S_i will first check its route cache to verify if there are existing paths to D_i. If there is no such path in the cache, S_i will start a route discovery process by broadcasting a RREQ packet. The channel-free probability $P_{\boldsymbol{p}_{i,j}}$ will also be recorded within the header of the RREQ packet. Recall that $P_{\boldsymbol{p}_{i,j}}$ from Equation (8) represents the probability that the channel along the considered path $\boldsymbol{p}_{i,j}$ is free to be utilized. Upon receiving the RREQ packet, the forwarding node $F_{i,j,k}$ will multiply $P_{\boldsymbol{p}_{i,j}}$ with its own channel idle probability $P^I_{F_{i,j,k}}$, which is obtained from its MAC layer protocol as in Equation (7). The channel-free probability $P_{\boldsymbol{p}_{i,j}}$ along the path $\boldsymbol{p}_{i,j}$ that is stored within the RREQ packet will consequently be updated, i.e., $P_{\boldsymbol{p}_{i,j}} = P_{\boldsymbol{p}_{i,j}} \cdot P^I_{F_{i,j,k}}$. The RREQ packet will be rebroadcasted if the path to the destination node is not available. Until D_i is first found in the route discovery process *via* a specific path $\boldsymbol{p}_{i,f}$, the first RREP packet will be initiated by D_i, and will be sent back to S_i *via* the reverse path, i.e., *via* the shortest path $\boldsymbol{p}_{i,f}$.

Moreover, at the time instant that the first RREQ packet has arrived in D_i, a timer will be initiated by the destination node D_i. As the timer expires, an additional RREP packet initiated by D_i to S_i is allowed in the proposed MCR algorithm, i.e., two reverse paths between the same source/destination pair. The criterion for sending the additional RREP packet from D_i holds if one of the latter paths has a larger channel-free probability compared with the first path $\boldsymbol{p}_{i,f}$, i.e.,

$$\boldsymbol{p}_{i,s} \triangleq \arg_{\boldsymbol{p}_{i,\varsigma}} \left\{ \max_{\forall \boldsymbol{p}_{i,\varsigma} \in \mathbf{P}_i, \varsigma \neq f} (P_{\boldsymbol{p}_{i,\varsigma}}) > P_{\boldsymbol{p}_{i,f}} \right\} \tag{9}$$

As a result, $\boldsymbol{p}_{i,s}$ is selected as the second path due to its larger $P_{\boldsymbol{p}_{i,s}}$ value compared with $P_{\boldsymbol{p}_{i,f}}$. Recall that the channel-free probabilities are accumulated along the path $\boldsymbol{p}_{i,s}$ *via* the RREQ packets. It will also be delivered back to S_i within the RREP packet via the reverse path $\boldsymbol{p}_{i,s}$. The source node S_i will first utilize the constructed path (i.e., *via* the shortest path $\boldsymbol{p}_{i,f}$) to initiate data transmission to D_i, while the second path (i.e., $\boldsymbol{p}_{i,s}$) may also be established afterwards. In general, the RREP packet *via* the path $\boldsymbol{p}_{i,s}$ will arrive in S_i in a latter time owing to the larger hop counts in the path. S_i will consequently change its data delivering path from $\boldsymbol{p}_{i,f}$ to $\boldsymbol{p}_{i,s}$ (if $\boldsymbol{p}_{i,s} \neq \emptyset$) in order to avoid the network congestion along the original path $\boldsymbol{p}_{i,f}$. Furthermore, as the hop counts of the first path are lower than that of the second path, an additional control message named the channel congestion test (CONG_TEST) packet will also be initiated by S_i towards the first path $\boldsymbol{p}_{i,f}$ in order to determine if the congestion problem along $\boldsymbol{p}_{i,f}$ has been resolved. This can be contributed to the termination of the interfering traffic that happens around the first path $\boldsymbol{p}_{i,f}$. The CONG_TEST message, which contains the value of $P_{\boldsymbol{p}_{i,s}}$ within its packet header, will be delivered along the path $\boldsymbol{p}_{i,f}$. A criterion is verified at each node $F_{i,f,k}$ within the path $\boldsymbol{p}_{i,f}$ to compare if its own channel idle probability ($P^I_{F_{i,f,k}}$) is greater than the threshold within the CONG_TEST message as

$$P^I_{F_{i,f,k}} \geq (P_{\boldsymbol{p}_{i,s}})^{\frac{1}{HC_{\boldsymbol{p}_{i,f}}}} \tag{10}$$

where $HC_{\boldsymbol{p}_{i,f}}$ represents the total hop counts along the path $\boldsymbol{p}_{i,f}$. If the condition on (10) is satisfied, the CONG_TEST message will be carried to the next hopping node along the path $\boldsymbol{p}_{i,f}$. After the message has arrived in D_i, it will be traversed back to S_i, which guarantees the resolution of the congestion problem along the path $\boldsymbol{p}_{i,f}$. Once S_i has detected the CONG_TEST message again, the data transmission from S_i will be adaptively switched back to the path $\boldsymbol{p}_{i,f}$, which at present is considered to be the path that has the lowered channel congestion with the smallest hop counts. Moreover, due to the limited numbers of the constructed route within the network, only a slightly amount of control packets will be incurred by the CONG_TEST messages.

In order to exactly consider the level of congestion with routing paths, it is intuitive that the criterion $P_{\boldsymbol{p}_{i,f}} \geq P_{\boldsymbol{p}_{i,s}}$ should be utilized instead of Equation (10), since it represents the comparison of channel idle probabilities between the two paths. However, this criterion is considered difficult to be implemented because it requires significant amount of control overheads to detect the actual congestion-free probabilities of both paths in real-time manner. Instead, the criterion in Equation (10) is adopted for the decision of path-switching. Once the channel-free probability of each node along the first path satisfies Equation (10), the first path is considered the path with better channel quality since it is supposed to possess higher congestion-free probability. More precisely, the correctness of path-switching criterion proposed in Equation (10) can be verified from Equation (8)

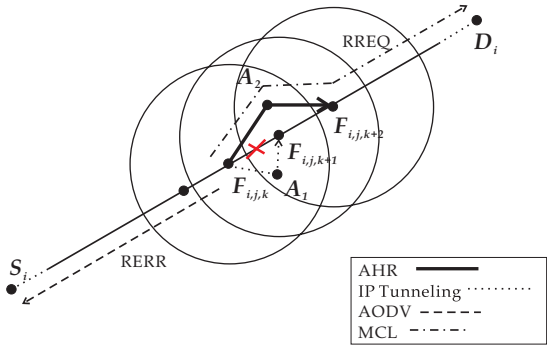

Figure 2. Schematic diagram for the route repair schemes.

as follows:

$$P_{\boldsymbol{p}_{i,f}} = \prod_{k=1}^{HC_{\boldsymbol{p}_{i,f}}} P^I_{F_{i,f,k}} \geq \prod_{k=1}^{HC_{\boldsymbol{p}_{i,f}}} (P_{\boldsymbol{p}_{i,s}})^{\frac{1}{HC_{\boldsymbol{p}_{i,f}}}} = P_{\boldsymbol{p}_{i,s}} \quad (11)$$

Therefore, the design of path-switching scheme in Equation (10) can provide fair congestion alleviation between routing paths for real-time implementation.

3.3. Aggressive hop-reduction (AHR) local repair

Route repair mechanism is required for multihop routing schemes since the communication links can be broken due to many factors, e.g., power exhaustion or unexpected shutdown of the WNs. In most of the congestion-controlled routing schemes, the selected route is in general not the shortest path in order to avoid the network congestion in certain areas. Excessive hop counts from the source to the destination node consequently result in degraded routing efficiency, i.e., with lowered packet delivery ratio and elongated routing delay. Therefore, it is necessary to provide an efficient route repair mechanism, i.e., the proposed AHR scheme such as to effectively reduce the total number of hop counts.

Figure 2 illustrates the route repair schemes that are utilized in different protocols. It is assumed that the communication link is broken between the forwarding nodes $F_{i,j,k}$ and $F_{i,j,k+1}$. The conventional AODV protocol utilizes the route error (RERR) packet for route repair. As node $F_{i,j,k}$ loses connectivity to its next hop, it will initiate an RERR packet back to the source node S_i to restart a new route discovery process. Local route repair scheme is adopted in the MCL protocol [10], where node $F_{i,j,k}$ will initiate a new route discovery process toward the unreachable destination D_i by sending the RREQ packet as shown in Figure 2. As can be expected, significant transmission delay will be observed with these two route repair schemes. The IP tunneling is utilized in Reference [18] to construct a new route between nodes $F_{i,j,k}$ and $F_{i,j,k+1}$. As a consequence, an additional hop count is expected (i.e., *via* node A_1) in order to reconnect nodes $F_{i,j,k}$ and $F_{i,j,k+1}$. It is predicted that the number of hop counts can be drastically augmented due to the increased amount of unreliable communication links.

The AHR scheme employed in the proposed MCR algorithm further reduces the total number of hop counts during the local repair phase. As the link between nodes $F_{i,j,k}$ and $F_{i,j,k+1}$ is broken, node $F_{i,j,k}$ will begin a new route discovery process toward both nodes $F_{i,j,k+1}$ and $F_{i,j,k+2}$. It is noticed that node $F_{i,j,k+2}$ is available to node $F_{i,j,k}$ since the next two-hop information is recorded in the routing table of a WN. Node $F_{i,j,k}$ will select the reconstructed local path with the smallest total number of hop counts. For example, two local paths are obtained by node $F_{i,j,k}$ as $[F_{i,j,k},\ A_2,\ F_{i,j,k+2}]$ and $[F_{i,j,k},\ A_1,\ F_{i,j,k+1},\ F_{i,j,k+2}]$. It is clear that the path $[F_{i,j,k},\ A_2,\ F_{i,j,k+2}]$ will be selected by node $F_{i,j,k}$ since it has comparably smaller number of hop counts. Moreover, it is noted that the broken links are detected based on the status of routing table in the AHR scheme. In other words, the inactiveness of a path in the routing table depends upon certain situations such as the lifetime of the routing table, and the unreachable next-hop while forwarding packets under severe congestions. The exploitation of periodic hello packets are not utilized in the AHR scheme due to its excessive control overheads. Furthermore, due to the localized behavior of the AHR scheme, the difference on the channel status is considered negligible between adjacent WNs. Therefore, the channel-free probability is not exploited in the AHR local path selection criterion.

3.4. Implementation of MCR algorithm

The proposed MCR scheme is considered to be implementable in an open source operating system, e.g., under the Linux environment. The netfilter hooks, which intercept and manipulate the incoming packets in Linux kernel, can be utilized to obtain the NAV information within the received RTS and CTS packets. Based on the availability of NAV vectors, the channel-busy probability for each node as defined in Equation (6) can therefore be computed.

Furthermore, the route discovery process as described in subsection 3.2 is designed to be a modified version of the conventional ADOV protocol, which has been realized in Linux kernel environment and released as an open source called Kernel AODV protocol. Both the RREQ and RREP packets in the Kernel AODV algorithm can carry the required information for the computation of channel-free probability that contributes to the fulfillment of proposed MCR protocol. By adjusting the Kernel AODV scheme, the proposed MCR algorithm can consequently be implemented as a Linux Kernel program.

4. ANALYTICAL MODELING OF PACKET DELIVERY RATIO

Analytical study is performed in order to explore the benefits of the proposed MCR protocol. There existing research

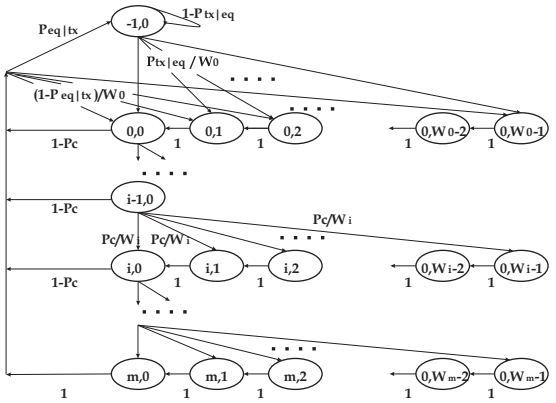

Figure 3. Embedded Markov chain model for IEEE 802.11 backoff mechanism.

[19–24] are establishing the analytical models for the IEEE 802.11 MAC protocol under certain assumptions. An IEEE 802.11 backoff model is proposed in Reference [19] under the saturation state, while the non-saturated model is presented in Reference [20]. Most of the related research are devoted on throughput analysis within the MAC layer. In this section, the backoff model of the IEEE 802.11 protocol [20] is extended and integrated with the M/M/1 queuing system [25] in order to explore the effect of the packet delivery ratio from the network layer perspective. It is noticed that the purpose of this section is not to propose a comprehensive analytical model, but to provide a methodology in order to analytically illustrate the effectiveness of the proposed MCR algorithm, i.e., to analytically indicate the influence from the network congestion that contains both effect of data rate/size and the number of interfering nodes. For simplicity, Poisson traffic that uniformly distributed among nodes is considered. Moreover, only the localized effect is taken into account in the derivation of the model, i.e., the routing performance within a single-hop between the WNs is studied. We notice that one hop effect in fact does not imply any topology of the network, e.g., a grid or totally symmetrical networks. The packet delivery ratio will, therefore, be obtained based on the proposed formulation. Consequently, the influence of the data rate and the number of the interfering neighbors will be investigated in the next section.

The embedded Markov chain of the IEEE 802.11 backoff mechanism is shown in Figure 3. The backoff timer at the ith stage can be represented as $W_i = 2^i \cdot W$, where W denotes the minimum contention window, and $i \in [0, m]$ with m represents the maximum backoff stage. As illustrated in Figure 3, the backoff state $(s(t), b(t))$ consists of two discrete-time stochastic processes, i.e., $s(t)$ indicates the backoff stage $i \in [0, m]$ and $b(t)$ denotes the backoff counter for each WN. It is also noted that the state $(-1, 0)$ is introduced on behalf of the empty queue within a WN. In order to facilitate the computation of the transition probability P_t, three associated probabilities are introduced as follows: (a) P_c: the packet collision probability, (b) $P_{tx|eq}$: the probability of an incoming transmission obtained after an empty queue in a WN, and (c) $P_{eq|tx}$: the probability of an empty queue is observed after a successful transmission or a maximum backoff. The values of these three probabilities will be computed later in this section. The stationary probabilities of each state $S_{i,k}$ with $i \in [0, m]$ and $k \in [0, W_i - 1]$ can concisely be represented as follows:

$$S_{-1,0} = \frac{P_{eq|tx}}{P_{tx|eq}} \cdot P_{\text{sum}} \tag{12}$$

$$S_{i,k} = \frac{W_i - k}{W_i} \cdot P_c^i \cdot S_{0,0} \quad k \in [0, W_i - 1], i \in [0, m] \tag{13}$$

where $P_{\text{sum}} = \sum_{i=0}^{m-1}(1 - P_c) \cdot S_{i,0} + S_{m,0}$. The derivations of Equations (12) and (13) can be obtained in Appendix A. As a consequence, the state probability $S_{0,0}$ is determined as

$$\begin{aligned} S_{0,0} &= \left(\sum_{i=0}^{m} \sum_{k=0}^{W_i - 1} \frac{W_i - k}{W_i} \cdot P_c^i + \frac{P_{eq|tx}}{P_{tx|eq}} \right)^{-1} \\ &= \left(\frac{1}{2} \left[\frac{1-(2P_c)^{m+1}}{1-2P_c} W_0 + \frac{1 - P_c^{m+1}}{1-P_c} \right] + \frac{P_{eq|tx}}{P_{tx|eq}} \right)^{-1}. \end{aligned} \tag{14}$$

On the other hand, the probability of any transmission within a WN in a randomly selected time slot, i.e., the conditional transition probability τ, can be expressed as

$$\tau = \sum_{i=0}^{m} S_{i,0} = \frac{1 - P_c^{m+1}}{1 - P_c} S_{0,0} \tag{15}$$

Assuming that there are α interfering neighbor nodes, the conditional packet collision probability P_c can, therefore, be obtained as

$$P_c = 1 - (1 - \tau)^{\alpha - 1} \tag{16}$$

After incorporating Equation (14) into Equations (15) and (16), the values of both P_c and τ can therefore be obtained, where $P_{tx|eq}$ and $P_{eq|tx}$ are described in Appendix B as the function of P_c and τ.

There are three different behaviors that can occur within a WN for handling an outgoing packet, including successful packet transmission, packet collision, and packet withdraw after the maximum retransmission. Therefore, the effective service rate μ_e can be represented as

$$\mu_e = (1 - P_c) \cdot \mu_s + P_w \cdot \mu_w + (P_c - P_w) \cdot \mu_c \tag{17}$$

where $P_w = P_c S_{m,0} / (\sum_{i=0}^{m} S_{i,0}) = [P_c^{m+1}(1 - P_c) S_{0,0}] / (1 - P_c^{m+1})$ is the probability of packet withdraw. The service rates for a successful transmission (μ_s), packet

withdraw (μ_w), and packet collision (μ_c) are expressed as

$$\mu_s = \left(T_s + \sum_{i=0}^{m} \frac{W_i - 1}{2} \cdot \overline{\sigma} \cdot \frac{P_c^i}{\sum_{j=0}^{m} P_c^j} \right)^{-1} \quad (18)$$

$$\mu_w = \left(T_c + \frac{W_m - 1}{2} \cdot \overline{\sigma} \right)^{-1} \quad (19)$$

$$\mu_c = \left(T_c + \sum_{i=0}^{m-1} \frac{W_i - 1}{2} \cdot \overline{\sigma} \cdot \frac{P_c^i}{\sum_{j=0}^{m-1} P_c^j} \right)^{-1} \quad (20)$$

In this paper, it is supposed as in Reference [20] that the input traffic and the network processing time follow the behavior of the M/M/1 model, where the effective service rate can be acquired as in Equation (17). By mapping the system into the M/M/1 queueing model, the complete rate for successful transmission becomes

$$\mathrm{CR}_s = \mathrm{E}[U] \cdot (1 - P_c)\mu_s = \rho \cdot (1 - P_c)\mu_s \quad (21)$$

where the expectation value of the queue utilization (U) is $\mathrm{E}[U] = \rho$ for the M/M/1 queueing system. Recall that the parameter ρ corresponds to the traffic intensity and is expressed as $\rho = \lambda/\mu_e$. As a result, the packet delivery ratio $\mathcal{R}$ can be obtained as

$$\mathcal{R} = \frac{\mathrm{CR}_s}{\lambda} = (1 - P_c) \cdot \frac{\mu_s}{\mu_e} \quad (22)$$

with μ_e and μ_s acquired from Equations (17) and (18). In the next section, the packet delivery ratio $\mathcal{R}$ will be utilized as the criterion for evaluating the network performance under different data rates and interfering neighbor nodes.

5. PERFORMANCE EVALUATION AND COMPARISON

In this section, the performance of the proposed MCR scheme is evaluated and compared *via* both the analytical study and the simulation results. The IEEE 802.11 DCF scheme is utilized as the MAC protocol, while the two-ray ground propagation model is employed in the simulations. The constant bit rate (CBR) is adopted as the traffic type, while both the transmission range and carrier sensing range for each WN are chosen as 100 m. The active time of a route is designed to be 40 s, which is comparably larger than the inter-arrival time of a packet plus the delay time. Therefore, the cache life time is considered to be sufficient in our simulation environment. The major reason is due to the objective of this paper which focuses on the alleviation of network congestion under more static environments. In order to provide feasible comparisons between different congestion-controlled algorithms, longer cache life time is adopted in order to prevent frequent reconstruction of routes. The following three criterions are utilized as the performance metrics:

(1) The Packet Delivery Ratio (%): The ratio of the number of the received data packets to the number of the total data packets sent by the sources.
(2) The Average End-to-End Delay (s): The average time elapsed for delivering a data packet within a successful transmission.
(3) The Control Overhead: The total number of required control packets.

Subsection 5.1 presents the determination of the time interval for computing the channel-busy probability. Subsection 5.2 describes the analytical study on the network performance considering the effects from both the data rate and the neighbor interference. The performance comparisons between the proposed MCR scheme and the existing protocols are illustrated in Subsection 5.3.

5.1. Determination of time interval ΔT

In order to obtain the channel-free probability $P_{\boldsymbol{p}_{i,j}}$ for the considered path in Equation (8), it is required to first compute the channel-busy probability P_k^B for each node k as in Equation (6). In other words, it is necessary to determine the feasible total number of time slots n in Equation (6) such that a stable time interval in consideration can be acquired, i.e., $\Delta T = n \cdot \sigma$. For implementation purpose, the parameter ΔT will be utilized as the time duration for observing the channel status, i.e., either in the busy or the idle state. In this paper, the DSSS (i.e., with $\sigma = 20\,\mu$s) is adopted both in the analysis and the simulations. We recall that the random variables $\mathcal{X}_i$ stated in subsection 3.1 are not independent of each other. The dependency between busy time slot and its sequent slot occurs since a busy time slot has high probability to result in a successive busy slot due to the unfinished packet transmission. On the other hand, the independency between the idle time slot and its following slot can be attributed to the unpredictable random back-off mechanism in the IEEE 802.11 protocol. However, based on the observations associated with the finite length of data packets, the corresponding channel condition set $\boldsymbol{X}$ can be considered as an M-dependent sequence [26]. Since such a sequence can be approximately independent as n is large enough than the dependent interval, the following property of convergence to the expectation value can be assured by adopting the law of large numbers, i.e.,

$$\lim_{n\to\infty} P_k^b = \lim_{n\to\infty} \frac{1}{n} \sum_{i=t}^{t-n} \mathcal{X}_i \to m_b \quad (23)$$

according to the large deviation as

$$P\left(\left| \frac{1}{n} \sum_{i=1}^{n} \mathcal{X}_i - m_b \right| > \varepsilon \right) \leq \beta^n + \hat{\beta}^n \quad (24)$$

where m_b is denoted as the mean value of $\boldsymbol{X}$. Intuitively, the randomness of P_k^b will decrease gradually as the

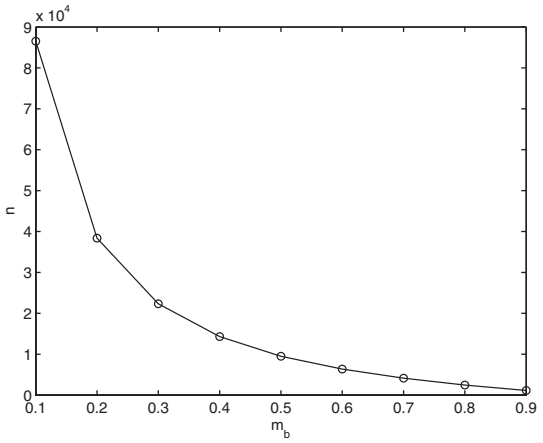

Figure 4. The relationship between the expected value of $\boldsymbol{X}$ (i.e., m_b) and the required number of time slots n.

sample size n is increased. In other words, the limit behavior will become more stable with a longer considered time interval. It is noticed that $\beta = \exp[-I_X(m_b + \varepsilon)]$ and $\hat{\beta} = \exp[-I_X(m_b - \varepsilon)]$, where ε indicates the tolerant error. $I_X(\xi)$ represents the large deviation rate function for $\boldsymbol{X}$, which is obtained as

$$I_X(\xi) = \sup_{\upsilon \in \mathbb{R}} [\upsilon \xi - C_X(\upsilon)] = \begin{cases} \xi \ln(\frac{\xi}{m_b}) + (1-\xi)\ln(\frac{1-\xi}{1-m_b}), & \text{if } 0 < \xi < 1 \\ -\ln(m_b), & \text{if } \xi = 1 \\ -\ln(1-m_b), & \text{if } \xi = 0 \\ \infty, & \text{otherwise} \end{cases} \tag{25}$$

where $C_X(\upsilon) = \ln[M_X(\upsilon)]$ denotes the cumulant generating function with the moment generating function $M_X(\upsilon)$ defined as

$$M_X(\upsilon) = \mathrm{E}[e^{\upsilon x}] = m_b e^{\upsilon} + 1 - m_b \tag{26}$$

The main concern is to obtain a feasible value of n such that P_k^B will approach the mean value m_b as in (23). Considering $P(\left|(1/n)\sum_{i=1}^{n} \mathcal{X}_i - m_b\right| > 0.04\, m_b) \leq 10^{-3}$ from Equation (24) as the criterion for acquiring the n value, the relationship between m_b and n can be illustrated as in Figure 4 from the range of $m_b = 0.1$ to 0.9. It can be observed that the maximum required number of time slots n is close to 10^5 in the $m_b = 0.1$ case. Therefore, the considered time interval ΔT for implementation can be computed as $\Delta T = n \cdot \sigma = 10^5 \times (20 \times 10^{-6}) = 2$ s by adopting the DSSS case. In other words, the current channel-busy probability is calculated according to samples in the past 2 s, i.e., by means of the sliding window with the window size of 2 s. Assuming that the maximum size of a packet is equal to 1024 bytes, the required transmission time of the packet can be found around 4–10 ms depending on both the channel bit rate and the propagation delay. It can be observed that the selected time interval $\Delta T = 2$ s is longer enough compared with the packet transmission time in order to support the convergent theory in Equation (23), while it is not too lengthy as being capable to capture the latest channel information. It is also noticed that different values of ΔT can be acquired with the similar procedures for other specifications. As a result, the DSSS system will be adopted in this paper associated with $\Delta T = 2$ s as the observation time interval in order to obtain the probability P_k^B in Equation (6) for the simulations in subsection 5.3.

Table I. Analytical and simulation parameters adopted from the DSSS system.

Parameter type	Parameter value
PHY header	128 bits
MAC header	272 bits
RTS frame size	160 bits + PHY header
CTS frame size	112 bits + PHY header
ACK frame size	112 bits + PHY header
Payload size of the data packet	1024 × 8 bits
Maximum backoff stages (m)	5
Minimum contention window (W)	32
Channel bit rate	1 Mbit/s
Slot time (σ)	20 μs
Propagation delay (T_δ)	1 μs
T_{SIFS}	10 μs
T_{DIFS}	50 μs

5.2. Analytical study on effects from data rate and neighbor interference

The network performance will be analyzed in this subsection by employing both the analytical and simulation results. The performance will be evaluated by considering the packet delivery ratio *versus* both the data rate and neighbor interference. Table I summarizes the parameters adopted from the DSSS system for both the analytical and the simulation results. The packet delivery ratio $\mathcal{R}$ computed from Equation (22) will be utilized as the analytical results, while the simulation results are conducted *via* the Network Simulator (ns-2; [27]). In order to illustrate that one transmission pair is interfered by another α pairs of packet delivery, the simulations are performed with $(\alpha + 1)$ pairs of WNs with point-to-point packet delivery. We also recall that the WNs possess the same transmission range with each other.

Before exploring the performance on the packet delivery ratio $\mathcal{R}$, an important parameter (i.e., the service time T_{sv} from (35)) will be investigated first. Figure 5 illustrates the comparison of T_{sv} *versus* the data rate (λ) and the number of interfering neighbors (α). As shown in both plots with lower data rate and smaller number of interfering neighbors, the value of service time (i.e., $T_{\mathrm{sv}} \approx 0.01$ s) is observed to be similar to the successful transmission time $T_s = 0.0094$ s, which can be calculated from (32) *via* the data from Table I.

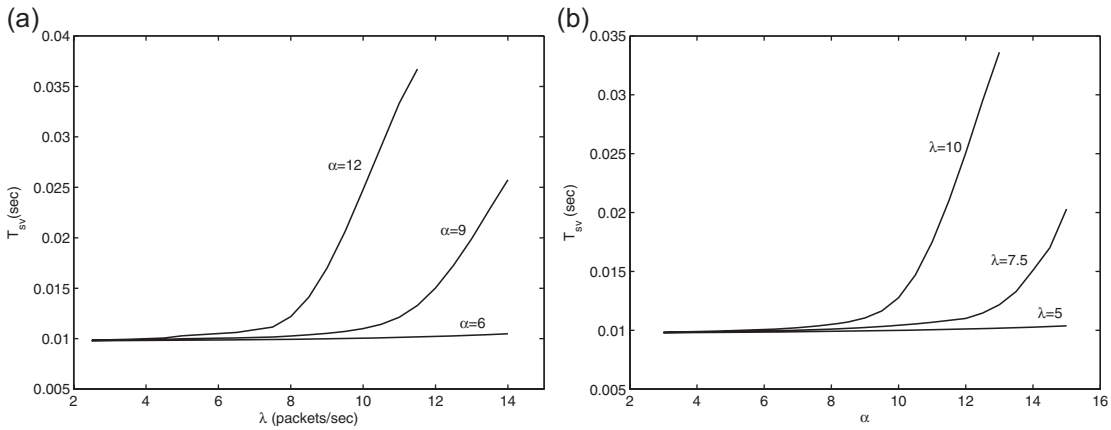

Figure 5. (a) Service time T_{sv} *versus* data rate λ; (b) Service time T_{sv} *versus* number of interfering neighbors α.

The results indicate that there is almost no packet collision under these situations, which make T_{sv} similar to T_s without the necessity for considering the backoff time in Equation (35). In most of the cases, however, the service time is perceived to significantly increase from a critical point (CP) either the data rate or the number of the interfering neighbors is augmented. The CP corresponds to the location of the capacity as $\mathcal{C} \triangleq 1/T_{sv}$, which is defined as the maximum services of the packets per unit time under the IEEE 802.11 MAC system. On the other hand, the total incoming packets per unit time obtained from the interfering neighbor nodes are computed as $\mathcal{T} = \lambda\alpha$. The reason for the drastic incline in both Figure 5(a) and (b) is mainly caused by the cases that the total interfering effect $\mathcal{T} = \lambda\alpha$ is around the same value or larger than the capacity $\mathcal{C}$. Due to the system saturation, the service time will be significantly increased since additional time is required for packet retransmission and collision. This assertion can also be validated by observing the CPs within Figure 5. The CP for $\alpha = 12$ and $\lambda = 7.5$ in Figure 5(a) (such that $\mathcal{T} = \lambda\alpha = 90$) corresponds to the capacity calculated as $\mathcal{C} = 91.07$, and the CP for $\lambda = 10$ and $\alpha = 9$ in Figure 5(b) (such that $\mathcal{T} = 90$) corresponds to $\mathcal{C} = 91.87$. Recall that $\mathcal{C} = 1/T_{sv}$, where the average service time T_{sv} is computed from Equation (35). It can be perceived that both $\mathcal{T}$ and $\mathcal{C}$ share the similar values in these cases, which validates the existence of the CP where the system saturation occurs.

Figure 6(a) shows the performance comparison for packet delivery ratio *versus* the data rates under $\alpha = 6$, 9, and 12, while Figure 6(b) illustrates the comparison for packet delivery ratio *versus* different numbers of interfering neighbors with $\lambda = 5$, 7.5, and 10. From both the plots, it can be observed that the analytical results are consistent with that acquired from the simulations, which validates the correctness of the derived analytical model. Similar to the observations from Figure 5(a) and (b), the performance degradation is perceived from the locations of the CP either the data rate or the number of the interfering neighbors is increased. As $\mathcal{T} < \mathcal{C}$, comparably higher packet delivery ratio $\mathcal{R}$ can be achieved since most of the packets can be successfully delivered without spending time for the retransmission process as is modeled in the Morkovian chain in Figure 3. On the other hand, as $\mathcal{T}$ reaches or exceeds the capacity $\mathcal{C}$, some of the packets will not be transmitted due to the system saturation that causes rapid decrease in the packet delivery ratio.

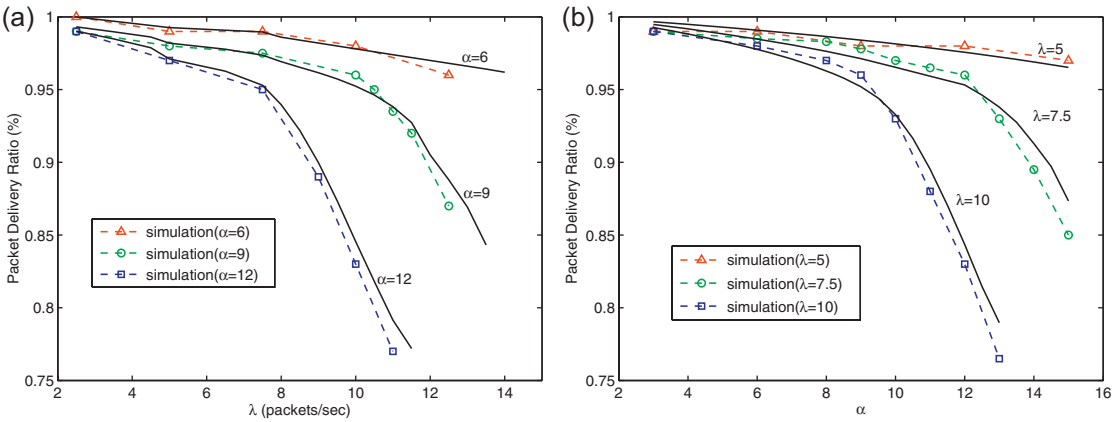

Figure 6. (a) Packet delivery ratio *versus* data rate λ; (b) Packet delivery ratio *versus* number of interfering neighbors α (Solid lines: analytical results; Dashed lines: simulation results).

Table II. Simulation parameters for the grid topology.

Parameter Type	Parameter Value
Data Rate	$\boldsymbol{p}_{1,j}$, $\boldsymbol{p}_{2,1}$: 5 packets/s
Size of Data Packet	$\boldsymbol{p}_{1,j}$, $\boldsymbol{p}_{2,1}$: 512 Bytes
	$\boldsymbol{p}_{3,1}$: 1024 Bytes
Transmission Time	$\boldsymbol{p}_{1,j}$: 400 ~ 1000 s
	$\boldsymbol{p}_{2,1}$, $\boldsymbol{p}_{3,1}$: 0 ~ 600 s
Total Simulation Time	1200 s

The occurrence of acute degradation of packet delivery ratio (as $\mathcal{T} < \mathcal{C}$) leads to the importance of designing a feasible routing algorithm for congestion control. The proposed MCR scheme estimates the level of network congestion *via* Equation (6), which implicitly considers the combining impact from both the data rate/size and number of interference neighbor nodes. It is especially noticed that the influence from the data rate/size has not been taken into account in previous network congestion studies [7–10]. Furthermore, the MCR algorithm is designed to adaptively select the routing path with diminished interfering effect, which inherently possesses smaller probability for packet collision. The total interfering effect from the neighboring nodes can be minimized such that the WNs within the route will not have much chance to reach their capacities $\mathcal{C}$. The proposed MCR scheme can, therefore, conduct the data delivery under the better network quality. Moreover, the performance study in this subsection only considers the localized effect for packet transmission with infinite data queue in each WN. The system saturation problem can become more severe by considering both the hidden terminal problem and the finite queuing effect under the multihop data delivery. We recall that the hidden terminal problem will further cause the interference from the two-hop away neighbor nodes. The substantial benefits of using the proposed MCR algorithm can become obvious under such realistic multihop environments. In the next subsection, the MCR scheme will be compared with other existing protocols *via* simulations under the environments of WMNs.

5.3. Performance comparison

The Network Simulator is utilized to implement and to compare the proposed MCR algorithm with the other existing routing schemes, including the AODV and the LBAR protocols. Both the grid and the random topologies are considered as the simulation scenarios for performance comparison.

5.3.1. The grid topology.

The grid topology as shown in Figure 7 is utilized as the first performance comparison for illustrating the process of adaptive path-switching. Table II shows the parameters that are adopted for the grid topology. As depicted in Figure 7, $\boldsymbol{p}_{2,1}$ and $\boldsymbol{p}_{3,1}$ are two existing route with their corresponding source/destination pairs, i.e., (S_2, D_2) and (S_3, D_3). The source node S_1 intends to initiate a new data transmission

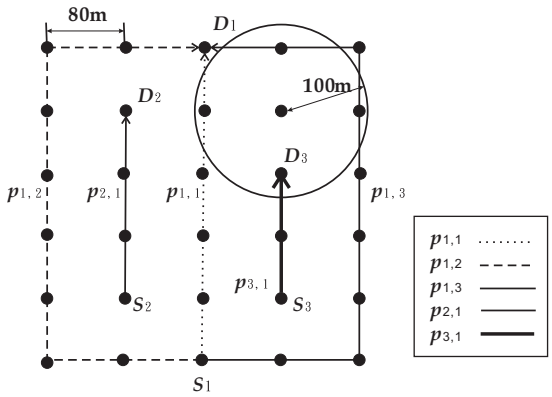

Figure 7. Schematic diagram of an exemplified grid network topology.

to the destination node D_1, where $\mathbf{P}_1 = \{\boldsymbol{p}_{1,j} \mid j = 1, 2, 3\}$ denotes the set of potential routes that can be selected according to different routing protocols. The transmission range of each WN encompasses its one-hop neighbor nodes as shown in Figure 7. As indicated in Table II, different data rates, data sizes, and starting time instants for data transmissions are utilized within the three different routes, i.e., $\boldsymbol{p}_{1,j}$, $\boldsymbol{p}_{2,1}$, and $\boldsymbol{p}_{3,1}$.

Figures 8–10 show the performance comparisons between the three schemes under different data rates (i.e., from 5 to 35 packets/s) along the route $\boldsymbol{p}_{3,1}$. It is noticed that $\boldsymbol{p}_{2,1}$ and $\boldsymbol{p}_{3,1}$ are the two existing routes for their corresponding data transmission. Both routes initiate their packet transmission earlier than $\boldsymbol{p}_{1,j}$ with distinct data rates as denoted in Table II. As can be seen from Figures 8 and 9 that the performance of the AODV protocol is severely degraded as the data rate of $\boldsymbol{p}_{3,1}$ is increased, i.e., with decreased packet delivery ratio and increased average end-to-end delay. The reason is primarily attributed to the reason that the total interfering effect $\mathcal{T}$ reaches the capacity $\mathcal{C}$ around the data rate of $\boldsymbol{p}_{3,1} = 15$ packets/s. The AODV protocol selects $\boldsymbol{p}_{1,1} \in \mathbf{P}_1$ for packet forwarding by using the shortest path criterion, which results in the significant net-

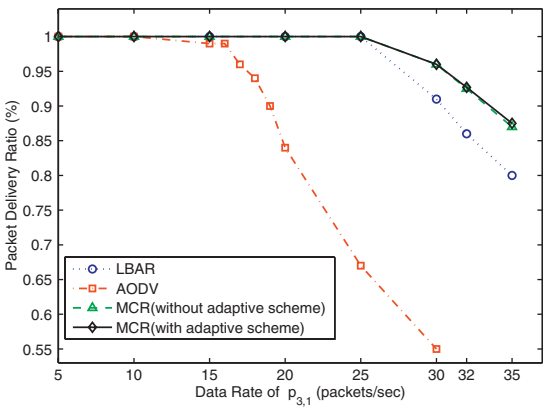

Figure 8. Simulation results of the grid topology: packet delivery ratio *versus* data rate of S_3.

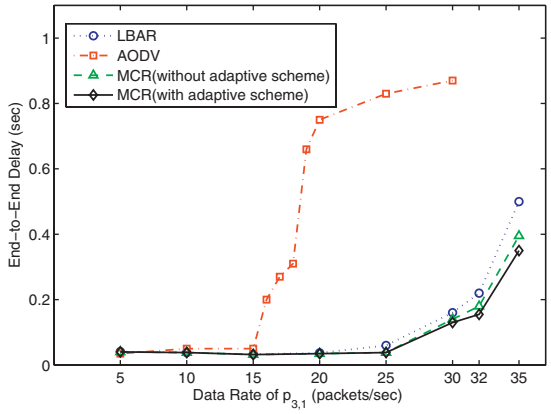

Figure 9. Simulation results of the grid topology: average end-to-end delay *versus* data rate of S_3.

work congestion from both the routes $\boldsymbol{p}_{2,1}$ and $\boldsymbol{p}_{3,1}$. On the other hand, the LBAR scheme conducts packet transmission using the path $\boldsymbol{p}_{1,3} \in \mathbf{P}_1$ since $\boldsymbol{p}_{1,3}$ is determined to have the smallest cost $\Omega_{\boldsymbol{p}_{1,3}}$ (as defined in Equation (1)) compared with $\boldsymbol{p}_{1,1}$ and $\boldsymbol{p}_{1,2}$. Reasonable routing performance can be observed using the LBAR scheme as shown in Figures 8 and 9. However, compared with the MCR and the AODV schemes as in Figure 10, the LBAR protocol costs substantial control packets for the computation of the cost function. Due to the excessive usage of the hello packets, around 2.5 order more of control overhead is observed by adopting the LBAR scheme. Moreover, the various data rates along different paths are not considered in the LBAR algorithm.

The proposed MCR protocol can provide better routing performance than the other two algorithms, e.g., around 5 and 40% more on the packet delivery ratio compared with the LBAR and the AODV schemes (under data rate = 30 packets/s). The path $\boldsymbol{p}_{1,1}$ will not be selected by the MCR scheme due to its severe network congestion problem. By adopting the MCR algorithm, the path selected within the set $\mathbf{P}_1$ may differ due to the various data rates that are possessed by its interfering neighbor nodes. As the data rate of $\boldsymbol{p}_{3,1}$ is lower than that of $\boldsymbol{p}_{2,1}$, the path $\boldsymbol{p}_{1,3}$ will be chosen owing to its least number of interfering neighbor nodes. On the other hand, the path $\boldsymbol{p}_{1,2}$ is selected while the data rate of $\boldsymbol{p}_{2,1}$ is comparably smaller than that of $\boldsymbol{p}_{3,1}$. Even though $\boldsymbol{p}_{1,3}$ has smaller interfering neighbor nodes, the high data rate associated with $\boldsymbol{p}_{3,1}$ can result in more severe packet collisions to the path $\boldsymbol{p}_{1,3}$. This reveals the reason for the MCR protocol to outperform the LBAR algorithm since the LBAR scheme still utilizes the path $\boldsymbol{p}_{1,3}$ even for its associated higher data rate. Consequently, it can be observed that the proposed MCR protocol selects the routing path by considering the effects from both the data rate and the interfering neighbor nodes.

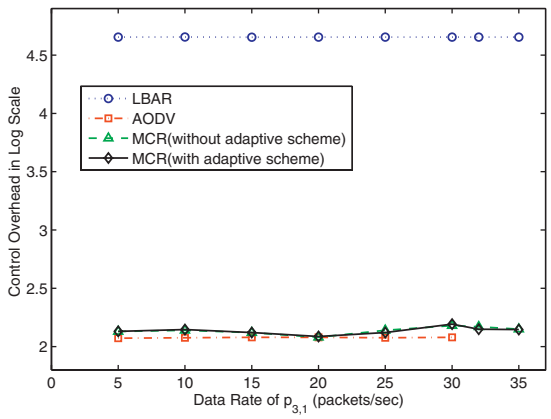

Figure 10. Simulation results of the grid topology: control overhead *versus* data rate of S_3.

Table III. Simulation parameters for the random topology.

Parameter Type	Parameter Value
Simulation Area	$5000 \times 2500\,\text{m}^2$
Number of Nodes	100
Maximum Transmission Time of Each Source	600 s
Total Simulation Time	1700 s

Moreover, the adaptive path-switching scheme within the MCR algorithm will adaptively change the routing path back to $\boldsymbol{p}_{1,1}$ while its interference is considered lower than the current transmitting path $\boldsymbol{p}_{1,2}$ or $\boldsymbol{p}_{1,3}$. By observing the simulation scenario, the MCR scheme changes the path back to $\boldsymbol{p}_{1,1}$ after $t > 600$ s, i.e., after the problem of the network congestion is improved due to the termination of $\boldsymbol{p}_{2,1}$ or $\boldsymbol{p}_{3,1}$. The adaptive path-switching mechanism can slightly alleviate the prolonged end-to-end delay (due to larger hop counts) that commonly occurred in the congestion-based routing algorithms. As shown in Figure 9, around 40 ms less delay is observed compared to that without the adaptive path-switching scheme under data rate = 35 packets/s. Furthermore, with the adoption of moderate amount of control packets (which are excessively utilized in the LBAR scheme), the MCR protocol prospects a routing path with lowered network interference by utilizing its inherent MAC capability, i.e., the NAV vectors obtained from both the RTS and the CTS packets.

5.3.2. The random topology.

The random topology is also utilized to evaluate the proposed MCR protocol, and the corresponding simulation parameters are shown in Table III. We recall that the starting time for packet transmission of each source node S_i is randomly selected between 0 and 1500 s, while the data size is randomly chosen between 512 and 1024 bytes.

Figures 11–13 show the performance comparison of these three protocols under (*i*) different numbers of source nodes (as in Figures 11(a), 12(a), and 13(a) with average[‡] data rate = 10 packets/s) and (*ii*) different average

[‡] The average data rate x indicates that the data rate of each route is randomly selected between 1 and $2x$.

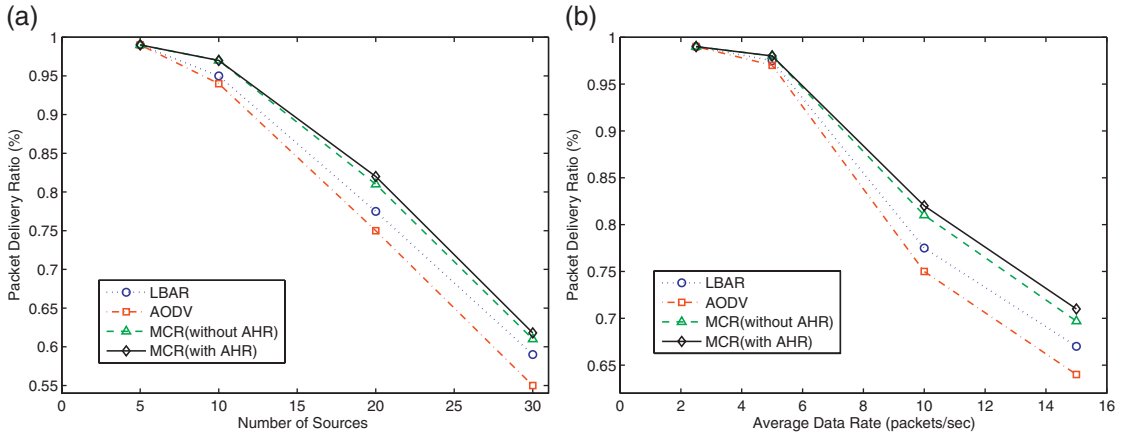

Figure 11. Simulation results of the random topology: (a) Packet delivery ratio *versus* number of sources; (b) Packet delivery ratio *versus* average data rate.

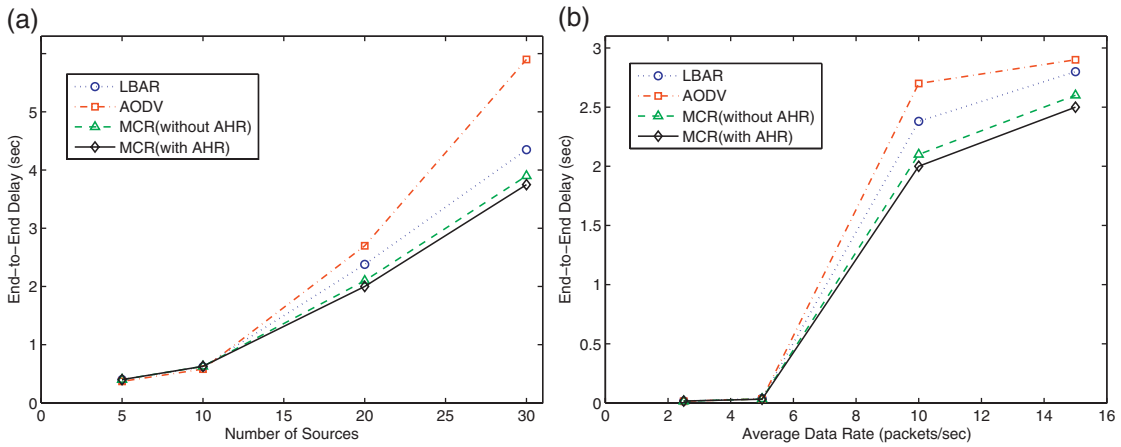

Figure 12. Simulation results of the random topology: (a) Average end-to-end delay *versus* number of sources; (b) Average end-to-end delay *versus* average data rate.

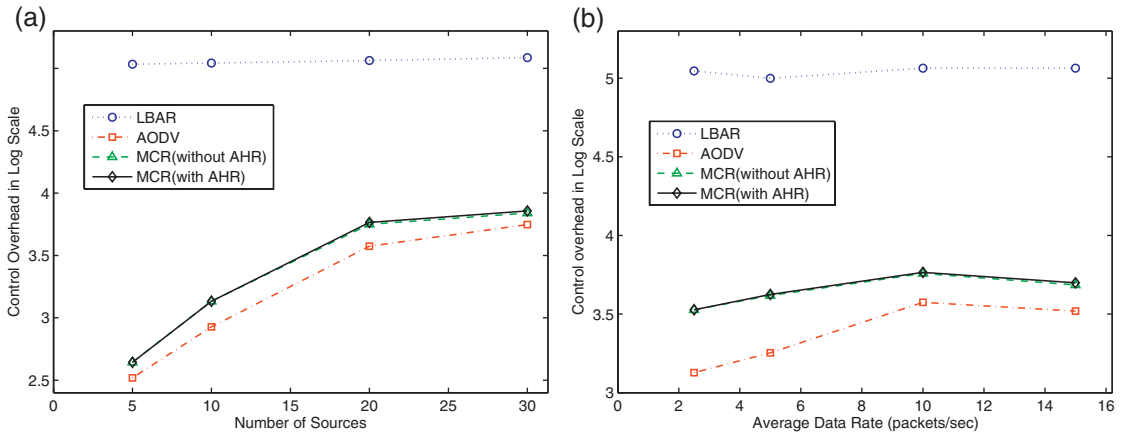

Figure 13. Simulation results of the random topology: (a) Control overhead *versus* number of sources; (b) Control overhead *versus* average data rate.

data rates (as in Figures 11(b), 12(b), and 13(b) with the number of source = 20). Note that the MCR without AHR scheme, as shown in Figures 11–13, conducts its local repair process by adopting the IP Tunneling method as described in subsection 3.3. It is observed that the proposed MCR algorithm outperforms the other two protocols with higher packet delivery radio and lower end-to-end delay. There are around 5 and 10% more in the packet delivery ratio and 0.5 and 2 s less in the end-to-end delay compared with the LBAR and the AODV methods (under the number of source node = 30 as in Figures 11 and 12). A comparably larger amount of routes selected by the MCR algorithm will not reach their capacities, which make the proposed scheme possesses better routing performance in average. Moreover, the accompanied AHR local repair process is advantageous as the conditions of network congestion becomes severe as shown in Figures 11 and 12.

It is observed from Figure 13 that the additional control overheads are induced in both the MCR and ADOV algorithms with the increased number of sources and averaged data rate. With a larger number of paths resulting from the augmented number of sources, additional control packets (e.g., the RREQ and RREP packets) are required for route discovery and construction. Moreover, higher data rate will, in general, leads to serious network congestion, which consequently results in more control packets for route repair. However, the control overheads obtained from both schemes are still comparably smaller than that from the LBAR protocol. Excessive control packets are utilized in the LBAR scheme for information exchange between the neighbor nodes in order to measure the network congestion level. As shown in Figure 13, the control packets that are utilized for route construction in the LBAR algorithm is considered negligible, which leads to its minor variations under different numbers of sources and data rates. Furthermore, compared with the AODV protocol, the reason why the MCR algorithm generates slightly more control packets is primarily due to additional usage of the RREQ packets in the route discovery process. However, the MCR protocol consumes significantly less control overhead than that from the LBAR algorithm, e.g., around 1.5 order less as in Figure 13(b) under different average data rates. The merits of using the MCR algorithm can be observed from these simulation results. The proposed MCR protocol can offer better routing performance even with the existence of network congestion.

6. CONCLUSION

An MCR protocol is proposed in this paper. The MCR algorithm incorporates the NAVs from the MAC protocol for the path determination within its route discovery processes. The proposed MCR protocol is accompanied with the adaptive path-switching scheme and the AHR local repair mechanism for the enhancement of network performance. The effectiveness of the proposed algorithm is evaluated *via* both the analytical study and the simulation results. Even with the network congestion, the routing performance can still be preserved by adopting the MCR protocol in the wireless multihop networks.

7. ACKNOWLEDGEMENT

This work was in part funded by the Aiming for the Top University and Elite Research Center Development Plan, NSC 96-2221-E-009-016, NSC 98-2221-E-009-065, the MediaTek research center at National Chiao Tung University, the Universal Scientific Industrial (USI) Co., and the Telecommunication Laboratories at Chunghwa Telecom Co. Ltd, Taiwan.

APPENDIX A

The transition probabilities in Figure 3 which are shortly denoted as $P_t(i_1, k_1 \mid i_0, k_0) \triangleq P_t(s(t+1) = i_1, b(t+1) = k_1 \mid s(t) = i_0, b(t) = k_0)$ can be obtained as follows:

$$\begin{cases} P_t(i, k \mid i, k+1) = 1 & k \in [0, W_i - 2], \quad i \in [0, m] \\ P_t(i, k \mid i-1, 0) = \dfrac{P_c}{W_i} & k \in [0, W_i - 1], \quad i \in [1, m] \\ P_t(-1, 0 \mid i, 0) = (1 - P_c) \cdot P_{eq\mid tx} & i \in [0, m-1] \\ P_t(-1, 0 \mid m, 0) = P_{eq\mid tx} & \\ P_t(0, k \mid i, 0) = \dfrac{(1 - P_c)(1 - P_{eq\mid tx})}{W_0} & k \in [0, W_0 - 1], \quad i \in [0, m-1] \\ P_t(0, k \mid m, 0) = \dfrac{1 - P_{eq\mid tx}}{W_0} & k \in [0, W_0 - 1] \\ P_t(0, k \mid -1, 0) = P_{tx\mid eq} \cdot \dfrac{1}{W_0} & k \in [0, W_0 - 1] \end{cases} \tag{27}$$

By defining the stationary distribution as $S_{i,k} = \lim_{t\to\infty} P_t(s(t) = i, b(t) = k)$ with $i \in [0, m]$ and $k \in [0, W_i - 1]$, the state probabilities can also be acquired from Figure 3 as

$$S_{0,k} = \frac{W_0 - k}{W_0}\left[S_{-1,0} \cdot P_{tx\mid eq} + (1 - P_{eq\mid tx}) P_{\text{sum}}\right] \quad k \in [0, W_i - 1] \tag{28}$$

$$S_{i,k} = \frac{W_i - k}{W_i} P_c \cdot S_{i-1,0} = \frac{W_i - k}{W_i} P_c^i \cdot S_{0,0} \quad k \in [0, W_i - 1],\ i \in [1, m] \tag{29}$$

$$S_{-1,0} = (1 - P_{tx\mid eq}) \cdot S_{-1,0} + P_{eq\mid tx} \cdot P_{\text{sum}} \tag{30}$$

APPENDIX B

Under the assumption of Poisson traffic with average data arrival rate λ (with unit as packets per second), the condi-

tional probability $P_{tx|eq}$ is acquired as

$$P_{tx|eq} = (1 - e^{-\lambda\sigma})(1 - \tau)^{\alpha-1} + (1 - e^{-\lambda T_{tx}})[1 - (1 - \tau)^{\alpha-1}] \quad (31)$$

where σ is the length of the slot time, and T_{tx} denotes the average transmission time as $T_{tx} = (1 - P_c) \cdot T_s + P_c \cdot T_c$. We recall that T_s represents the time required for a successful transmission, while T_c is the time for packet collision, i.e.,

$$T_s = T_{\text{RTS}} + T_{\text{CTS}} + T_\vartheta + T_{\text{ACK}} + 3T_{\text{SIFS}} + T_{\text{DIFS}} + 4T_\delta \quad (32)$$

$$T_c = T_{\text{RTS}} + T_{\text{DIFS}} + T_\delta \quad (33)$$

where T_δ denotes the propagation delay. The parameters T_ϑ, T_{RTS}, T_{CTS}, and T_{ACK} are the time required respectively for a data packet, for a RTS packet, for a CTS packet, and for an acknowledgement. T_{SIFS} and T_{DIFS} indicate the time intervals of the interframe space as defined in the IEEE 802.11 protocol. Moreover, with the consideration of moderate traffic load, the conditional probability $P_{eq|tx}$ can be obtained similar to the concept in [23] as

$$P_{eq|tx} = e^{-\lambda T_{\text{sv}}} \quad (34)$$

where the average service time, including both the backoff and the transmission states, of a packet is expressed as

$$T_{\text{sv}} = \sum_{i=0}^{m-1} \left[\frac{P_c^i}{\sum_{j=0}^{m} P_c^j} (1 - P_c) \left(T_s + iT_c + \sum_{k=0}^{i} \frac{W_k - 1}{2} \overline{\sigma} \right) \right] + \frac{P_c^m}{\sum_{j=0}^{m} P_c^j} \left[T_s(1 - P_c) + P_c T_c + mT_c + \sum_{k=0}^{m} \frac{W_k - 1}{2} \overline{\sigma} \right] \quad (35)$$

with the average time between the successive backoff timers denoted as $\overline{\sigma} = \sigma(1 - \tau)^{\alpha-1} + T_{tx} \cdot \left[1 - (1 - \tau)^{\alpha-1}\right]$.

REFERENCES

1. Gruber I, Bandouch G, Li H. *Ad hoc* routing for cellular coverage extension. *Proceedings of IEEE VTC*, 2003; 1816–1820.
2. Ding Z, Leung KK. Cross-layer routing optimization for wireless networks with cooperative diversity. *Proceedings of IEEE PIMRC*, 2008; 1–5.
3. Yang G, Shukla V, Qiao D. Analytical study of collaborative information coverage for object detection in sensor networks. *Proceedings of IEEE SECON*, 2008; 144–152.
4. Perkins CE, Bhagwat P. Highly dynamic destination-sequenced distance-vector routing (DSDV) for mobile computers. *Proceedings of ACM SIGCOMM*, 1994; 234–244.
5. Perkins C, Royer E. *Ad hoc* on-demand distance vector routing. *Proceedings of IEEE WMCSA*, 1999; 90–100.
6. Johnson DB, Maltz DA. Dynamic source routing in *ad hoc* wireless networks. *Mobile Computing*, 1996; 90–100.
7. Fang Y, McDonald AB. Dynamic codeword routing (DCR): a cross-layer approach for performance enhancement of general multi-hop wireless routing. *Proceedings of IEEE SECON*, 2004; 255–263.
8. Hassanein H, Zhou A. Routing with load balancing in wireless *ad hoc* networks. *Proceedings of ACM MSWiM*, 2001; 89–96.
9. Lee SJ, Gerla M. Dynamic load-aware routing in *ad hoc* networks. *Proceedings of IEEE ICC*, vol. 10, 2001; 3206–3210.
10. Kim BC, Lee JY, Lee HS, Ma JS. An *ad hoc* routing protocol with minimum contention time and load balancing. *Proceedings of IEEE GLOBECOM*, vol. 1, 2003; 81–85.
11. Presti FL. Joint congestion control, routing and media access control optimization *via* dual decomposition for *ad hoc* wireless networks. *Proceedings of ACM MSWiM*, 2005; 298–306.
12. Cao M, Raghunathan V, Kumar PR. Distributed energy aware cross-layer resource allocation in wireless networks. *Proceedings of WICON*, vol. 7, 2007.
13. Choi W, Das SK. Design and performance analysis of a proxy-based indirect routing scheme in *ad hoc* wireless networks. *Journal of MONET* 2003; **8**(5): 499–515.
14. Shekhar HMP, Ramanatha KS. Mobile agents based framework for routing and congestion control in mobile *ad hoc* networks. *Proceedings of CoNEXT*, 2006; 27.
15. Ahmed AU, Saito S, Cheng Z, Takizawa M. Zone-based congestion detection and control using routing method on the internet. *Journal of IJHPCN* 2007; **5**(1/2): 12–23.
16. Liu Z, Kwiatkowska MZ, Constantinou C. A biologically inspired congestion control routing algorithm for MANETs. *Proceedings of IEEE PerCom*, 2005; **5**(1/2)226–231.
17. Society IC. IEEE Standard 802.11: wireless LAN medium access control (MAC) and physical layer (PHY) specifications. *The Institute of Electrical and Electronics Engineers*, 1997.
18. Zhang X, Jacob L. Multicast zone routing protocol in mobile *ad hoc* wireless networks. *Proceedings of IEEE LCN*, 2003; 150–159.
19. Bianchi G. Performance analysis of the IEEE 802.11 distributed coordination function. *IEEE Journal on Selected Areas in Communication* 2000; **18**: 535–547.
20. Liaw YS, Dadej A, Jayasuriya A. Performance analysis of IEEE 802.11 DCF under limited load. *Proceedings of IEEE APCC*, 2005; 759–763.

21. He J, Kaleshi D, Munro A, *et al*. Performance investigation of IEEE 802.11 MAC in multihop wireless networks. *Proceedings of ACM/IEEE MSWIM*, 2005; 242–249.
22. Tickoo O, Sikdar B. Modeling and analysis of traffic characteristics in IEEE 802.11 MAC based networks. *Proceedings of IEEE GLOBECOM*, vol. 1, 2002; 67–71.
23. Alizadeh-Shabdiz F, Subramaniam S. Analytical models for single-hop and multi-hop *ad hoc* networks. *ACM/Springer Mobile Networks and Applications Journal* 2006; **11**: 75–90.
24. Wang Y, Garcia-Luna-Aceves JJ. Collision avoidance in multi-hop *ad hoc* networks. *Proceedings of IEEE MASCOTS*, pp. 145–154, 2002.
25. Gross D, Harris G. *Fundamentals of Queueing Theory* (3rd edn). Wiley: New Jersey, NY, USA, 1998.
26. Billingsley P. *Probability and Measure* (3rd edn). Wiley, 1995.
27. Heidemann J, Bulusu N, Elson J, *et al*. Effects of detail in wireless network simulation. *Proceedings of SCS Multiconference on Distributed Simulation*, 2001; 3–11.

AUTHORS' BIOGRAPHIES

Kai-Ten Feng received the BS degree from National Taiwan University, Taipei, in 1992, the MS degree from the University of Michigan, Ann Arbor, in 1996, and the PhD degree from the University of California, Berkeley, in 2000.

Since August 2007, he has been with the Department of Electrical Engineering, National Chiao Tung University, Hsinchu, Taiwan, as an associate professor. He was an assistant professor with the same department between February 2003 and July 2007. He was with the OnStar Corp., a subsidiary of General Motors Corporation, as an in-vehicle development manager/ senior technologist between 2000 and 2003, working on the design of future Telematics platforms and the in-vehicle networks. His current research interests include cooperative and cognitive networks, mobile ad hoc and sensor networks, embedded system design, wireless location technologies, and Intelligent Transportation Systems (ITSs).

He received the Best Paper Award from the IEEE Vehicular Technology Conference Spring 2006, which ranked his paper first among the 615 accepted papers. He is also the recipient of the Outstanding Young Electrical Engineer Award in 2007 from the Chinese Institute of Electrical Engineering (CIEE). He has served on the technical program committees of VTC, ICC, and APWCS.

Yu-Pin Hsu received the BS and MS degree both in the Department of Communication Engineering from the National Chiao-Tung University, Hsinchu, Taiwan, in 2005 and 2007 respectively. He was with the Center for Information and Communications Technology in the National Chiao-Tung University, as a research assistant between July 2007 and August 2009. Since September 2009, he has been working toward the PhD degree with the Department of Electrical and Computer Engineering from the Texas A&M University, U.S.A.. His current research interests include network coding and network information theory.